

Fig. 4. (Left) geometry of the perspective zenithal projections: (right) the three important special cases.

#### 4.1.1. AZP: perspective zenithal

Perspective zenithal projections are generated from a point and carried through the sphere to the plane of projection as illustrated in Fig. 4. We need consider only the case where the plane of projection is tangent to the sphere at its pole; the projection is simply rescaled if the plane intersects some other parallel of native latitude. If the source of the projection is at a distance  $\mu$  from the centre of the sphere ( $\mu > 0$  in the direction away from the plane of projection), then it is straightforward to show that

$$R_\theta = \frac{180^\circ}{\pi} \frac{\mu + 1}{\mu + \sin \theta} \cos \theta. \quad (16)$$

The inverse of this equation is

$$\theta = \arg(\rho, 1) - \sin^{-1} \left( \frac{\rho \mu}{\sqrt{\rho^2 + 1}} \right), \quad (17)$$

where

$$\rho = \frac{\pi}{180^\circ} \frac{R_\theta}{\mu + 1}.$$

The FITS keyword `PVj_1s`, attached to *latitude* coordinate  $j$ , will be used to specify  $\mu$  and the FITS projection type will be represented by the code AZP.

A *near-sided* perspective projection may be obtained with  $\mu < -1$ . This correctly represents the image of a sphere, such as a planet, when viewed from a distance  $|\mu|$  times the planetary radius. The coordinates of the reference point may be expressed in planetary longitude and latitude,  $(\lambda, \beta)$ . Also, the signs of the relevant elements of the `CDj-is` matrix may be chosen so that longitude increases as appropriate for a sphere seen from the outside rather than from within. A first-order correction for planetary oblateness may also be applied through the `CDj-is` matrix.

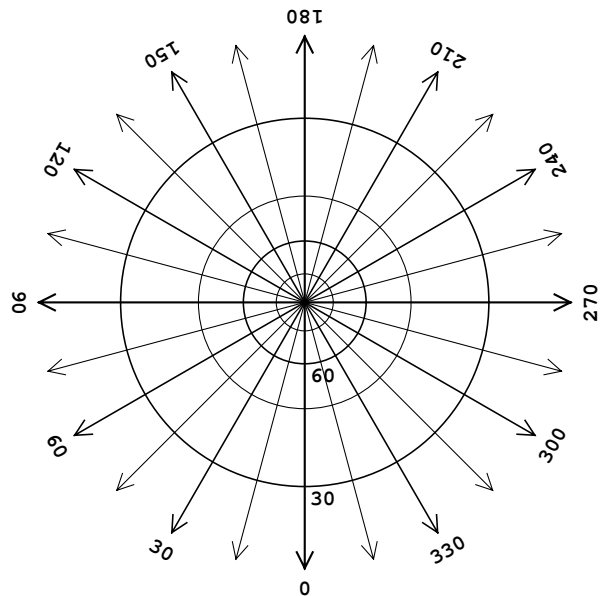


Fig. 5. Gnomonic projection; diverges at  $\theta = 0$ .

#### 4.1.2. TAN: gnomonic

The perspective zenithal projection with  $\mu = 0$ , the gnomonic<sup>5</sup> is widely used in optical astronomy and was given its own code within the AIPS convention, namely TAN<sup>6</sup>. For  $\mu = 0$  Eq. (16) reduces to

$$R_\theta = \frac{180^\circ}{\pi} \cot \theta, \quad (18)$$

with inverse

$$\theta = \tan^{-1} \left( \frac{180^\circ}{\pi R_\theta} \right). \quad (19)$$

<sup>5</sup> The gnomonic projection is the oldest known, dating to Thales of Miletus (ca. 624-547 B.C.). The stereographic and orthographic date to Hipparchus (ca. 190-after 126 B.C.).

<sup>6</sup> Referring to the dependence of  $R_\theta$  on the angular separation between the tangent point and field point, i.e. the native co-latitude.

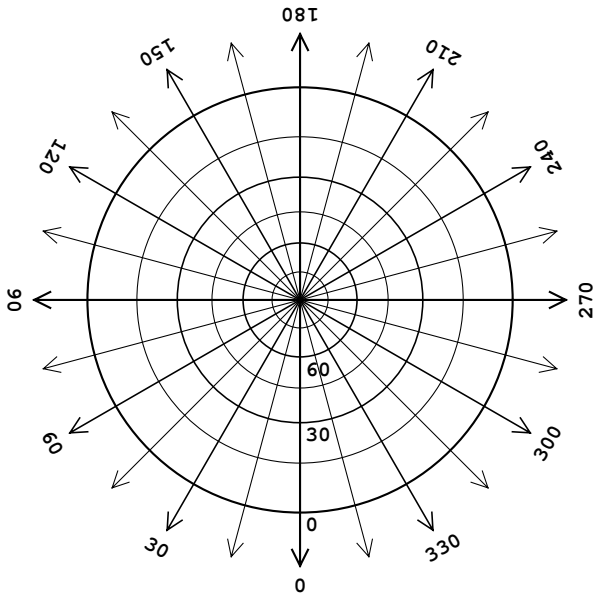


**Fig. 6.** Stereographic (STG) projection; diverges at  $\theta = -90^\circ$ .

The gnomonic projection is illustrated in Fig. 5. Since the projection is from the centre of the sphere, all great circles are projected as straight lines. Thus, the shortest distance between two points on the sphere is represented as a straight line interval, which, however, is not uniformly divided. The gnomonic projection diverges at  $\theta = 0$ , but one may use a gnomonic projection onto the six faces of a cube to display the whole sky. See Sect. 4.6.1 for details.

#### 4.1.3. STG: stereographic

The stereographic projection, the second important special case of the perspective zenithal projection defined by the AIPS convention, has  $\mu = 1$ , for which Eq. (16) becomes

$$\begin{aligned} R_\theta &= \frac{180^\circ}{\pi} \frac{2 \cos \theta}{1 + \sin \theta}, \\ &= \frac{360^\circ}{\pi} \tan \left( \frac{90^\circ - \theta}{2} \right), \end{aligned} \quad (20)$$

with inverse

$$\theta = 90^\circ - 2 \tan^{-1} \left( \frac{\pi R_\theta}{360^\circ} \right). \quad (21)$$

As first realized by astronomer Edmond Halley (1656-1742), the stereographic projection illustrated in Fig. 6 is the conformal (orthomorphic) zenithal projection, everywhere satisfying the requirement for conformality of zenithal projections:

$$\frac{\partial R_\theta}{\partial \theta} = \frac{-\pi R_\theta}{180^\circ \cos \theta}. \quad (22)$$

It also has the amazing property that it maps all circles on the sphere to circles in the plane of projection. Note, however, that concentric circles on the sphere are not necessarily concentric in the plane of projection.

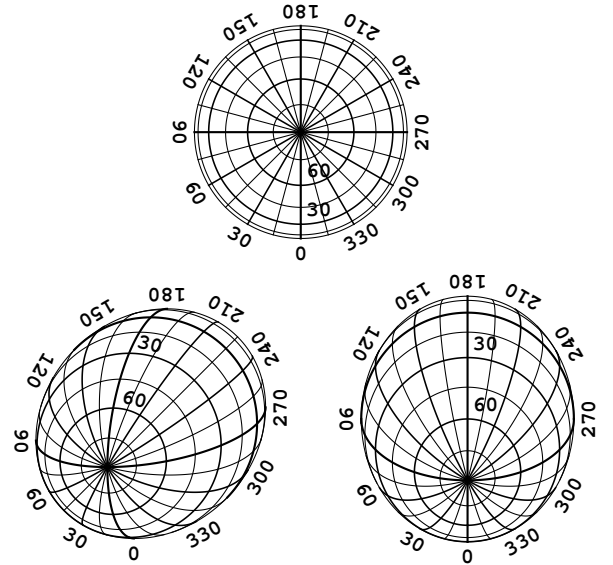


**Fig. 7.** Slant orthographic (SIN) projection: (top) the orthographic projection,  $\xi = 0, \eta = 0$ , north and south sides begin to overlap at  $\theta = 0$ ; (bottom left)  $Z = 30^\circ, \chi = 45^\circ$ ; (bottom right) projection appropriate for an east-west array observing at  $\delta_0 = 60^\circ$ .

#### 4.1.4. SIN: slant orthographic

The perspective zenithal projection with  $\mu = \infty$ , the orthographic, is illustrated in the upper portion of Fig. 7 (at consistent scale). It represents the visual appearance of a sphere, e.g. a planet, when seen from a great distance.

The orthographic projection is widely used in aperture synthesis radioastronomy and was given its own code within the AIPS convention, namely SIN<sup>7</sup>. Use of this projection code obviates the need to specify an infinite value as a parameter of AZP. In this case, Eq. (16) becomes

$$R_\theta = \frac{180^\circ}{\pi} \cos \theta, \quad (23)$$

with inverse

$$\theta = \cos^{-1} \left( \frac{\pi}{180^\circ} R_\theta \right). \quad (24)$$

In fact, use of the orthographic projection in radio interferometry is an approximation, applicable only for small field sizes. However, an exact solution exists where the interferometer baselines are co-planar. It reduces to what Greisen (1983) called the NCP projection for the particular case of an East-West interferometer as considered by Brouw (1971). This ‘‘slant orthographic’’ projection is a simple extension of the above formulæ

$$x = \frac{180^\circ}{\pi} [\cos \theta \sin \phi + \xi (\sin \theta - 1)], \quad (25)$$

$$y = -\frac{180^\circ}{\pi} [\cos \theta \cos \phi + \eta (\sin \theta - 1)], \quad (26)$$

It can be shown that these equations describe the case where the point of projection lies off the central axis of

<sup>7</sup> Similar etymology to TAN.

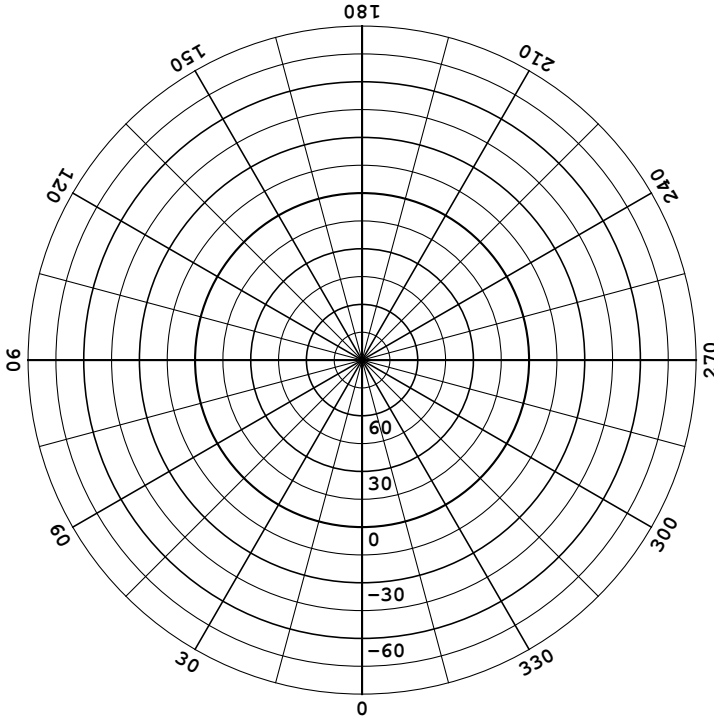


Fig. 8. Zenithal equidistant (ARC) projection; no limits.

the generating sphere and that the result is equivalent to an orthographic projection which has been stretched in one direction. We therefore extend the SIN projection to encompass it, with  $\xi$  and  $\eta$  given by keywords PVj\_1s and PVj\_2s, respectively, attached to *latitude* coordinate  $j$ .

The relationship between  $(\xi, \eta)$  and the native coordinates,  $(\phi_c, \theta_c)$ , of the central point of the projection is

$$\begin{aligned} \xi &= \cot \theta_c \sin \phi_c, \\ \eta &= \cot \theta_c \cos \phi_c, \end{aligned} \quad (27)$$

or

$$\begin{aligned} \phi_c &= 180^\circ + \arg(\eta, \xi), \\ \theta_c &= \tan^{-1} \left( \frac{1}{\sqrt{\xi^2 + \eta^2}} \right). \end{aligned} \quad (28)$$

The outer boundary of the SIN projection is given by

$$\theta_{\text{bound}} = \tan^{-1} (\xi \sin \phi + \eta \cos \phi). \quad (29)$$

Appendix D derives and discusses the slant orthographic projection in a radioastronomy context. Two example graticules are illustrated in the lower portion of Fig. 7.

#### 4.1.5. ARC: zenithal equidistant

Some non-perspective zenithal projections are also of interest in astronomy. The zenithal equidistant projection first appeared in Greisen (1983) as ARC. It is widely used as the approximate projection of Schmidt telescopes. As illustrated in Fig. 8, the native meridians are uniformly divided to give equi-spaced parallels. Thus

$$R_\theta = 90^\circ - \theta, \quad (30)$$

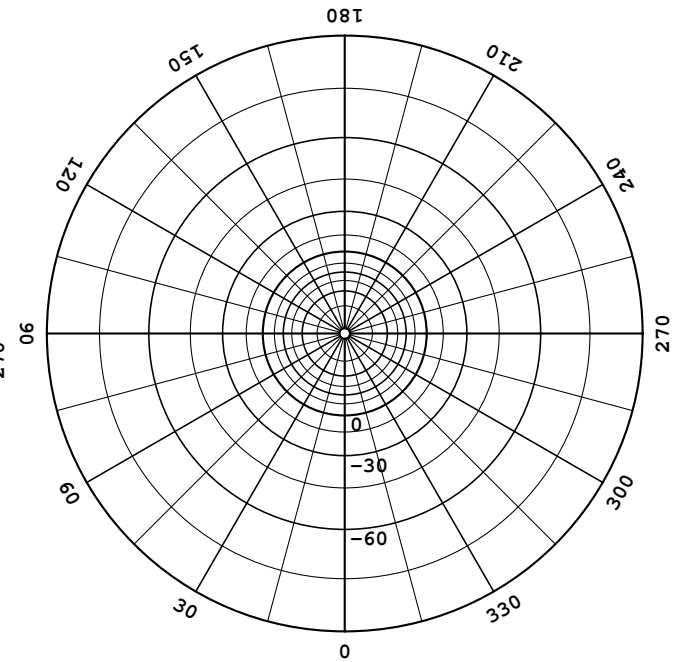


Fig. 9. Zenithal polynomial projection (ZPN) with parameters, 0.050, 0.975, -0.807, 0.337, -0.065, 0.010, 0.003, -0.001; limits depend upon the parameters.

which is trivially invertible. This projection was also known in antiquity.

#### 4.1.6. ZPN: zenithal polynomial

The zenithal polynomial projection, ZPN, generalizes the ARC projection by adding polynomial terms up to a large degree in the zenith distance. We define it as

$$R_\theta = \frac{180^\circ}{\pi} \sum_{i=0}^{99} P_i \left( \frac{\pi}{180^\circ} (90^\circ - \theta) \right)^i. \quad (31)$$

Note the units implied by the  $\frac{\pi}{180^\circ}$ . It is not immediately clear why  $P_0$  would ever be set non-zero, however we do not dismiss it as a possibility. Since its inverse cannot be expressed analytically, this projection should only be used when the geometry of the observations require it. In particular, it should never be used as an  $n^{\text{th}}$ -degree expansion of one of the standard zenithal projections.

The  $P_i$  are given by the keywords PVj\_0s, PVj\_1s, ..., PVj\_99s, attached to *latitude* coordinate  $j$ , all of which have default values of zero. An example of this projection is illustrated in Fig. 9.

#### 4.1.7. ZEA: zenithal equal-area

Lambert's zenithal equal-area projection illustrated in Fig. 10 is constructed by defining  $R_\theta$  so that the area enclosed by the native parallel at latitude  $\theta$  in the plane of projection is equal to the area of the corresponding spherical cap. It may be generated using

$$R_\theta = \frac{180^\circ}{\pi} \sqrt{2(1 - \sin \theta)} \quad (32)$$

**Table 5.** Second example FITS header (blank lines have been inserted for clarity).

123456789	123456789	123456789	123456789	123456789	123456789	123456789	123456789
NAXIS	=		2	/	2-dimensional image		
NAXIS1	=		2048	/	x axis (fastest)		
NAXIS2	=		2048	/	y axis (2nd fastest)		
MJD-OBS	=	44258.7845612		/	MJD at start of observation		
CD1_1	=		-0.005	/	Transformation matrix element		
CD1_2	=		0.00002	/	Transformation matrix element		
CD2_1	=		-0.00001	/	Transformation matrix element		
CD2_2	=		0.005	/	Transformation matrix element		
PV2_1	=		-25.0	/	Conic mid-latitude		
CRPIX1	=		1024.5	/	Pixel coordinate of reference point		
CRPIX2	=		-1023.5	/	Pixel coordinate of reference point		
CTYPE1	=	'GLON-COE'		/	Conic equal area projection		
CTYPE2	=	'GLAT-COE'		/	Conic equal area projection		
CRVAL1	=		90.0	/	Galactic longitude at reference point		
CRVAL2	=		-25.0	/	Galactic latitude at reference point		
CD1_1A	=		-0.005	/	Transformation matrix element		
CD1_2A	=		0.00002	/	Transformation matrix element		
CD2_1A	=		-0.00001	/	Transformation matrix element		
CD2_2A	=		0.005	/	Transformation matrix element		
PV2_1A	=		-25.0	/	Conic mid-latitude		
CRPIX1A	=		1024.5	/	Pixel coordinate of reference point		
CRPIX2A	=		-1023.5	/	Pixel coordinate of reference point		
CTYPE1A	=	'ELON-COE'		/	Conic equal area projection		
CTYPE2A	=	'ELAT-COE'		/	Conic equal area projection		
CRVAL1A	=		-7.0300934	/	Ecliptic longitude at reference point		
CRVAL2A	=		34.8474143	/	Ecliptic latitude at reference point		
LONPOLEA	=		6.3839706	/	Native longitude of ecliptic pole		
LATPOLEA	=		29.8114400	/	Ecliptic latitude of native pole		
RADESYS	=	'FK5'		/	Mean IAU 1984 ecliptic coordinates		

and (10) must therefore be used to obtain  $(\ell_p, b_p) = (-90^\circ, 90^\circ)$ . The galactic coordinates of the field point listed in Table 6 are then readily obtained by application of Eqs. (2).

The header says that the ecliptic coordinates of the reference point are  $(\lambda_0, \beta_0) = (-7^\circ 0300934, 34^\circ 8474143)$  and the native longitude of the ecliptic pole is  $\phi_p = 6^\circ 3839706$ . It also specifies LATPOLEA as  $29^\circ 8114400$ . In this case Eq. (8) has two valid solutions,  $\beta_p = -25^\circ 1367794 \pm 54^\circ 9482194$ , and the one closest in value to LATPOLEA (in fact equal to it) is chosen. If LATPOLEA had been omitted from the header its default value of  $+90^\circ$  would have selected the northerly solution anyway, but of course it is good practice to make the choice clear. The value of  $\lambda_p$  may be obtained by a straightforward application of Eqs. (9) and (10), and the ecliptic coordinates of the field point computed via Eqs. (2) are listed in Table 6 as the final step of the calculation. The reader may verify the calculation by transforming the computed galactic coordinates of the field point to mean ecliptic coordinates.

**Table 6.** Working for example 2.

$(p_1, p_2)$	1957.2	775.4
$(x, y)$	$-4^\circ 6275220$	$8^\circ 9851730$
$\theta_a, \eta$	$-25^\circ 0000000$	$0^\circ 0000000$
$\theta_1, \theta_2$	$-25^\circ 0000000$	$-25^\circ 0000000$
$\gamma$	$-0.8452365$	
$C, Y_0$	$-0.4226183$	$-122^\circ 8711957$
$(\phi, \theta)$	$-4^\circ 7560186$	$-15^\circ 8973800$
$(\ell_p, b_p)$	$-90^\circ 0000000$	$90^\circ 0000000$
$(\ell, b)$	$85^\circ 2439814$	$-15^\circ 8973800$
$(\lambda_p, \beta_p)$	$-179^\circ 9767827$	$29^\circ 8114400$
$(\lambda, \beta)$	$-14^\circ 7066741$	$43^\circ 0457292$

### 6.5. Header interpretation example 3

This example has been adapted from a real-life FITS data file written by a popular image analysis system. The simplicity of the header shown in Table 7 is deceptive; it is actually presented as an example of how *not* to write a FITS header, although the latent problem with its interpretation is quite subtle.

**Table 7.** Third example FITS header.

123456789	123456789	123456789	123456789	123456789	123456789	123456789	123456789
NAXIS	=	2	/	2-dimensional image			
NAXIS1	=	181	/	x axis (fastest)			
NAXIS2	=	91	/	y axis (2nd fastest)			
CD1_1	=	-1.0	/	Transformation matrix element			
CD1_2	=	0.0	/	Transformation matrix element			
CD2_1	=	0.0	/	Transformation matrix element			
CD2_2	=	1.0	/	Transformation matrix element			
CRPIX1	=	226.0	/	Pixel coordinate of reference point			
CRPIX2	=	46.0	/	Pixel coordinate of reference point			
CTYPE1	=	'GLON-CAR'		/ Plate carree projection			
CTYPE2	=	'GLAT-CAR'		/ Plate carree projection			
CRVAL1	=	30.0	/	Galactic longitude at reference point			
CRVAL2	=	35.0	/	Galactic latitude at reference point			

Observe that the image spans  $180^\circ$  in native longitude and  $90^\circ$  in native latitude and that the reference pixel lies outside the image. In fact, the reference pixel is located so that the native longitude runs from  $45^\circ$  to  $225^\circ$  and hence the image lies partly inside and partly outside the normal range of native longitude,  $[-180^\circ, 180^\circ]$ .

In fact, as might be expected, this makes no difference to the computation of celestial coordinates. For example, in computing the celestial coordinates of pixel (1, 1) we readily find from Eqs. (46) and (47) that the native coordinates are  $(\phi, \theta) = (225^\circ, -45^\circ)$ . The fact that  $\phi$  exceeds  $180^\circ$  becomes irrelevant once Eqs. (2) are applied since the trigonometric functions do not distinguish between  $\phi = 225^\circ$  and  $\phi = -135^\circ$ . The latter value is the appropriate one to use if the cylinder of projection is considered to be “rolled out” over multiple cycles. Consequently the correct galactic coordinates are obtained.

So where is the problem? It surfaces when we come to draw a coordinate grid on the image. A meridian of longitude, for example, is traced by computing the pixel coordinates for each of a succession of latitudes along the segment of the meridian which crosses the image. As usual, in computing pixel coordinates, the celestial coordinates are first converted to native coordinates by applying Eqs. (5) and herein lies the rub; the native longitude will be returned in the normal range  $[-180^\circ, 180^\circ]$ . Consequently, in those parts of the image where  $\phi > 180^\circ$  the pixel coordinates computed will correspond to the point at  $\phi - 360^\circ$ , i.e. in the part of the principle cycle of the cylindrical projection outside the image.

In principle it is possible to account for this, at least in specific cases, particularly for the cylindrical projections which are somewhat unusual in this regard. In practice, however, it is difficult to devise a general solution, especially when similar problems may arise for projection types where it is not desirable to track  $\phi$  outside its normal range. For example, consider the case where an Aitov projection is used to represent the whole sky; since its boundary is curved there will be out-of-bounds areas in the corner of the image. Normally a grid drawing rou-

tine can detect these by checking whether the inverse projection equations return a value for  $\phi$  outside its normal range. It may thus determine the proper boundary of the projection and deal with the discontinuity which arises when a grid line passes through it.

How then should the header have been written? Note that the problem exists at the lowest level of the coordinate description, in the conversion between  $(x, y)$  and  $(\phi, \theta)$ , and the solution must be found at this level. The problem arose from a particular property of cylindrical projections in that they have  $x \propto \phi$ . We must use this same property, which we might call  $\phi$ -translation invariance, to recast the coordinate description into a more manageable form.  $\phi$ -translation invariance simply means that changing the origin of  $\phi$  corresponds to shifting the image in the  $x$ -direction. In other words, we can transfer the reference point of the projection from its current location to another location along the native equator without having to regrid the image. The fact that the  $CDj\_is$  matrix is unity in this example makes this task a little simpler than otherwise.

Note first that because the image straddles  $\phi = 180^\circ$  we can't simply reset CRPIX1 so as to shift the reference point to  $\phi = -360^\circ$ ; the image would then straddle  $\phi = -180^\circ$  which is no improvement. In this example it is convenient and sufficient to shift the reference point to  $(\phi, \theta) = (-180^\circ, 0^\circ)$  which corresponds to pixel coordinate  $(p_1, p_2) = (46.0, 46.0)$ . Hence we need to reset CRPIX1 to 46.0 and adjust the keywords which define the celestial coordinate system. The reader may readily verify that the galactic coordinates of the new reference point are  $(\ell, b) = (210^\circ, -35^\circ)$  and whereas the old, implied value of LONPOLE was  $0^\circ$  when  $\delta_0 > 0$ , now that  $\delta_0 < 0$  its new implied value is  $180^\circ$ , and this is correct. However, we will set it explicitly anyway. The keywords to be changed are therefore

```
CRPIX1 = 46.0,
CRVAL1 = 210°,
CRVAL2 = -35°,
```

LONPOLE = 180° ,

What if the  $CDj_{-is}$  matrix was not unity? The problem of determining the pixel coordinates where  $(\phi, \theta) = (-180^\circ, 0^\circ)$  would have presented little extra difficulty, although in general CRPIX2 would also need to be changed. On reflection it may come as a surprise that changing the CRPIX $i$  like this does not fundamentally alter the linear transformation. However it may readily be verified that the only effect of changing the CRPIX $i$  is to change the origin of the  $(x, y)$  coordinates.

### 6.6. Header construction example 1

The following example comes from the  $4096 \times 4096$  pixel SFD infrared dust maps produced by Schlegel et al. (1998). The authors chose to regrid data from the COBE/DIRBE and IRAS/ISSA maps onto two zenithal equal area (ZEA) projections centered on the galactic poles. The projection formula given in their appendix C expressed in terms of standard 1-relative FITS pixel coordinates  $(p_1, p_2)$  is

$$\begin{aligned} p_1 - 1 &= 2048\sqrt{1 - n \sin b} \cos \ell + 2047.5, \\ p_2 - 1 &= -n2048\sqrt{1 - n \sin b} \sin \ell + 2047.5, \end{aligned}$$

where  $n = +1$  for the NGP and  $n = -1$  for the SGP maps. Now for ZEA from Eqs. (1), (12), (13), and (32)

$$\begin{aligned} CD1.1(p_1 - CRPIX1) &= \sqrt{2} \frac{180^\circ}{\pi} \sqrt{1 - \sin \theta} \sin \phi, \\ CD2.2(p_2 - CRPIX2) &= -\sqrt{2} \frac{180^\circ}{\pi} \sqrt{1 - \sin \theta} \cos \phi. \end{aligned}$$

If we take the NGP case first, the SFD equations may be rewritten as

$$\begin{aligned} p_1 - 2048.5 &= -2048\sqrt{1 - \sin b} \sin(\ell - 90^\circ), \\ p_2 - 2048.5 &= -2048\sqrt{1 - \sin b} \cos(\ell - 90^\circ). \end{aligned}$$

By inspection of the two sets of equations we must have

$$\begin{aligned} NAXIS &= 2, \\ NAXIS1 &= 4096, \\ NAXIS2 &= 4096, \\ CRPIX1 &= 2048.5, \\ CRPIX2 &= 2048.5, \\ CD1.1 &= -180^\circ \sqrt{2}/(2048\pi), \\ CD2.2 &= 180^\circ \sqrt{2}/(2048\pi), \\ CTYPER1 &= 'GLON-ZEA', \\ CTYPER2 &= 'GLAT-ZEA', \\ \ell &= \phi + 90^\circ, \\ b &= \theta. \end{aligned}$$

Now, writing  $\ell$  and  $b$  in place of  $\alpha$  and  $\delta$  in Eqs. (2), we have to determine  $\ell_p$ ,  $b_p$  and  $\phi_p$  to give  $(\ell, b)$  in terms of

$(\phi, \theta)$ . This is easy because we know  $b_p = 90^\circ$  and the simple special case Eqs. (3) apply so

$$\ell = \phi + (\ell_p - \phi_p - 180^\circ).$$

We have a degree of freedom here since only  $\ell_p - \phi_p$  is determined. It's best to let  $\phi_p$  take its default value which is  $0^\circ$  for zenithal projections with the celestial pole at the native pole (it's  $180^\circ$  otherwise), so we must have

$$\begin{aligned} CRVAL1 &= 270^\circ, \\ CRVAL2 &= 90^\circ, \\ LONPOLE &= 0^\circ. \end{aligned}$$

Although LONPOLE assumes its default value here it would of course be wise to write it explicitly into the header. The procedure for the SGP case is similar. The SFD equations may be rewritten

$$\begin{aligned} p_1 - 2048.5 &= 2048\sqrt{1 - \sin(-b)} \sin(90^\circ - \ell), \\ p_2 - 2048.5 &= 2048\sqrt{1 - \sin(-b)} \cos(90^\circ - \ell), \end{aligned}$$

whence

$$\begin{aligned} CRPIX1 &= 2048.5, \\ CRPIX2 &= 2048.5, \\ CD1.1 &= 180^\circ \sqrt{2}/(2048\pi), \\ CD2.2 &= -180^\circ \sqrt{2}/(2048\pi), \\ \ell &= 90^\circ - \phi, \\ b &= -\theta. \end{aligned}$$

Equations (4) apply for  $b_p = -90^\circ$  so

$$\ell = (\ell_p + \phi_p) - \phi.$$

Again we let  $\phi_p$  take its default value of  $180^\circ$ , so

$$\begin{aligned} CRVAL1 &= 270^\circ, \\ CRVAL2 &= -90^\circ, \\ LONPOLE &= 180^\circ. \end{aligned}$$

It's generally easier to interpret coordinate headers than to construct them so it's essential after formulating the header to test it at a few points and make sure that it works as expected. Note that this sort of translation exercise wouldn't be necessary if the formalism of this paper was used right from the start, i.e. in the regridding operation used to produce the maps.

### 6.7. Header construction example 2

Consider now the coordinate description for the two-dimensional image formed by a long slit spectrograph. We assume that the wavelength axis of length 1024 and dispersion  $\Delta\lambda$  nm/pixel corresponds to the  $p_1$  pixel coordinate, and the 2048 pixel spatial axis corresponds to  $p_2$ . The slit is centred on equatorial coordinates  $(\alpha_0, \delta_0)$  and oriented at position angle  $\rho$  measured such that when  $\rho = 0$  the first spectrum is northwards. We will assume that the telescope and spectrograph optics are such that the distance

keywords shown here are used to specify the minimum and maximum legal values in XPOS and YPOS columns and are useful for determining the range of each axis when constructing the image histogram.

## Appendix B: Mathematical methods

### B.1. Coordinate rotation with matrices

The coordinate rotations represented in Eqs. (2) or (5) may be represented by a matrix multiplication of a vector of direction cosines. The matrix and its inverse (which is simply the transpose) may be pre-computed and applied repetitively to a variety of coordinates, improving performance. Thus, we have

$$\begin{pmatrix} l \\ m \\ n \end{pmatrix} = \begin{pmatrix} r_{11} & r_{12} & r_{13} \\ r_{21} & r_{22} & r_{23} \\ r_{31} & r_{32} & r_{33} \end{pmatrix} \begin{pmatrix} l' \\ m' \\ n' \end{pmatrix}, \quad (\text{B.1})$$

where

$$\begin{aligned} l' &= \cos \delta \cos \alpha \\ m' &= \cos \delta \sin \alpha \\ n' &= \sin \delta \\ l &= \cos \theta \cos \phi \\ m &= \cos \theta \sin \phi \\ n &= \sin \theta \\ r_{11} &= -\sin \alpha_p \sin \phi_p - \cos \alpha_p \cos \phi_p \sin \delta_p \\ r_{12} &= \cos \alpha_p \sin \phi_p - \sin \alpha_p \cos \phi_p \sin \delta_p \\ r_{13} &= \cos \phi_p \cos \delta_p \\ r_{21} &= \sin \alpha_p \cos \phi_p - \cos \alpha_p \sin \phi_p \sin \delta_p \\ r_{22} &= -\cos \alpha_p \cos \phi_p - \sin \alpha_p \sin \phi_p \sin \delta_p \\ r_{23} &= \sin \phi_p \cos \delta_p \\ r_{31} &= \cos \alpha_p \cos \delta_p \\ r_{32} &= \sin \alpha_p \cos \delta_p \\ r_{33} &= \sin \delta_p. \end{aligned}$$

The inverse equation is

$$\begin{pmatrix} l' \\ m' \\ n' \end{pmatrix} = \begin{pmatrix} r_{11} & r_{21} & r_{31} \\ r_{12} & r_{22} & r_{32} \\ r_{13} & r_{23} & r_{33} \end{pmatrix} \begin{pmatrix} l \\ m \\ n \end{pmatrix}. \quad (\text{B.2})$$

### B.2. Iterative solution

Iterative methods are required for the inversion of several of the projections described in this paper. One, Mollweide's, even requires solution of a transcendental equation for the forward equations. However, these do not give rise to any particular difficulties.

On the other hand, it sometimes happens that one pixel and one celestial coordinate element is known and it is required to find the others; this typically arises when plotting graticules on image displays. Although analytical solutions exist for a few special cases, iterative methods must be used in the general case. If, say,  $i_1$  and  $\alpha_1$

are known, one would compute the pixel coordinate as a function of  $\delta$  and determine  $\delta_1$  as the value for which  $i = i_1$ . The unknown pixel coordinate elements would be obtained in the process.

This prescription glosses over many complications, however. All bounded projections may give rise to discontinuities in the graph of  $i$  versus  $\delta$  (to continue the above example), for example where the  $\alpha_1$  meridian crosses the  $\phi = \pm 180^\circ$  boundary in cylindrical, conic and other projections. Even worse, if the meridian traverses a pole represented as a finite line segment then  $i$  may become multi-valued at a particular value of  $\delta$ . The derivative  $\partial i / \partial \delta$  will also usually be discontinuous at the point of discontinuity, and it should be remembered that some projections such as the quad-cubes may also have discontinuous derivatives at points within their boundaries.

We will not attempt to resolve these difficulties here but simply note that WCSLIB (Calabretta, 1995) implements a solution.

## Appendix C: Projection aliases

Table C.1 provides a list of aliases which have been used by cartographers for special cases of the projections described in Sect. 4.

## Appendix D: The slant orthographic projection

The slant orthographic or generalized SIN projection derives from the basic interferometer equation (e.g. Thompson et al., 1986). The phase term in the Fourier exponent is

$$\varphi = (\mathbf{e} - \mathbf{e}_0) \cdot \mathbf{B}, \quad (\text{D.1})$$

where  $\mathbf{e}_0$  and  $\mathbf{e}$  are unit vectors pointing towards the field centre and a point in the field,  $\mathbf{B}$  is the baseline vector, and we measure the phase  $\varphi$  in rotations so that we don't need to carry factors of  $2\pi$ . We can write

$$\varphi = p_u u + p_v v + p_w w, \quad (\text{D.2})$$

where  $(u, v, w)$  are components of the baseline vector in a right-handed coordinate system with the  $w$ -axis pointing from the geocentre towards the source and the  $u$ -axis lying in the equatorial plane, and

$$\begin{aligned} p_u &= \cos \theta \sin \phi, \\ p_v &= -\cos \theta \cos \phi, \\ p_w &= \sin \theta - 1, \end{aligned} \quad (\text{D.3})$$

are the coordinates of  $(\mathbf{e} - \mathbf{e}_0)$ , where  $(\phi, \theta)$  are the longitude and latitude of  $\mathbf{e}$  in the spherical coordinate system with the pole towards  $\mathbf{e}_0$  and origin of longitude towards negative  $v$ , as required by Fig. 3. Now, for a planar array we may write

$$n_u u + n_v v + n_w w = 0 \quad (\text{D.4})$$

where  $(n_u, n_v, n_w)$  are the direction cosines of the normal to the plane. Using this to eliminate  $w$  from Eq. (D.2) we have

**Table C.1.** Projection aliases.

Name	Alias for	Name	Alias for
Gnomonic = Central	AZP with $\mu = 0$	Miller	CAR with $x$ scaled by $2/\pi$
Near-sided perspective	AZP with $\mu = 1.35$	Equiarectangular	CAR with unequal scaling
Clarke's (first)	AZP with $\mu = 1.35$	Cartesian	CAR
Clarke's (second)	AZP with $\mu = 1.65$	= Equidistant cylindrical	
James'	AZP with $\mu = 1.367$	Cassini	CAR transverse case
La Hire's	AZP with $\mu = 1.71$	Transverse Mercator	MER transverse case
Approximate equidistant zenithal	AZP with $\mu = 1.7519$	= Transverse cylindrical orthomorphic	
Approximate equal area zenithal	AZP with $\mu = 2.4142$	Sinusoidal	SFL
Postel	ARC	= Global sinusoid (GLS)	
= Equidistant		= Mercator equal-area	
= Globular		= Mercator-Sanson	
Lambert azimuthal equivalent	ZEA	= Sanson's	
= Lambert azimuthal equal area		Craster	PAR
= Lambert polar azimuthal		Bartholomew's atlantis	MOL oblique case
= Lorgna		Mollweide's homolographic	MOL
Gall's cylindrical	CYP with $\mu = 1, \lambda = \sqrt{2}/2$	= Homolographic	
Cylindrical equal area	CYP with $\mu = \infty$	= Homalographic	
Simple cylindrical	CYP with $\mu = 0, \lambda = 1$	= Babinet	
= Central cylindrical		= Elliptical	
= Cylindrical central perspective		Hammer equal area	AIT
= Gall's stereographic		= Aitoff	
Lambert's cylindrical	CYP with $\mu = \infty, \lambda = 1$	= Aitov	
= Lambert's equal area		Bartholomew's nordic	AIT oblique case
Behrmann equal area	CEA with $\lambda = 3/4$	One-standard conic	Conic with $\theta_1 = \theta_2$
Gall's orthographic	CEA with $\lambda = 1/2$	= Tangent conic	
= Approximate Peter's		Two-standard conic	Conic with $\theta_1 \neq \theta_2$
Lambert's equal area	CEA with $\lambda = 1$	= Secant conic	
		Murdoch conic	similar to COD
		Alber's	COE
		= Alber's equal area	
		Lambert equal area	COE with $\theta_2 = 90^\circ$
		Lambert conformal conic	for spherical Earth = COO
		Werner's	BON with $\theta_1 = 90^\circ$

$$\varphi = [p_u - \frac{n_u}{n_w} p_w]u + [p_v - \frac{n_v}{n_w} p_w]v \quad (\text{D.5})$$

Being the Fourier conjugate variables, the quantities in brackets become the Cartesian coordinates, in radians, in the plane of the synthesized map. Eqs (25) and (26) are then readily derived from Eqs. (D.3) and (D.5), and in the process we also obtain the following interpretation of the projection parameters

$$\begin{aligned} \xi &= n_u/n_w, \\ \eta &= n_v/n_w. \end{aligned} \quad (\text{D.6})$$

For an East-West interferometer,  $(\xi, \eta) = (0, \cot \delta_0)$ , while Cornwell & Perley (1992) give, for any instant of time,  $(\xi, \eta) = (\tan Z \sin \chi, \tan Z \cos \chi)$ , where  $Z$  is the zenith angle and  $\chi$  is the parallactic angle.

In synthesizing a map a phase shift may be applied to the visibility data in order to translate the field centre. If the shift applied is

$$\Delta\varphi = q_u u + q_v v + q_w w \quad (\text{D.7})$$

where  $(q_u, q_v, q_w)$  is constant then equation (D.2) becomes

$$\varphi = (p_u - q_u)u + (p_v - q_v)v + (p_w - q_w)w, \quad (\text{D.8})$$

whence equation (D.5) becomes

$$\varphi = [(p_u - q_u) - \xi(p_w - q_w)]u + [(p_v - q_v) - \eta(p_w - q_w)]v. \quad (\text{D.9})$$

Equations (25) and (26) become

$$\begin{aligned} x &= \frac{180^\circ}{\pi} ([\cos \theta \sin \phi + \xi(\sin \theta - 1)] - [q_u - \xi q_w]), \\ y &= -\frac{180^\circ}{\pi} ([\cos \theta \cos \phi + \eta(\sin \theta - 1)] - [q_v - \eta q_w]), \end{aligned} \quad (\text{D.10})$$

from which we see that the field centre is shifted by

$$\begin{aligned} \Delta x &= \frac{180^\circ}{\pi} (q_u - \xi q_w), \\ \Delta y &= \frac{180^\circ}{\pi} (q_v - \eta q_w). \end{aligned} \quad (\text{D.11})$$

The shift is applied to the coordinate reference pixel.